

# Modeling the scattering properties of particle suspensions in Singapore coastal waters with an analytic phase function

Boredin SAENGTUKSIN<sup>a,1</sup>, Chew Wai CHANG<sup>a,2</sup>, Soo Chin LIEW<sup>a,3</sup>

<sup>a</sup> Centre for Remote Imaging, Sensing and Processing (CRISP),  
National University of Singapore, 10 Lower Kent Ridge Road, Blk S17 Level 2, Singapore 119076

<sup>1</sup> Email: [boredin@nus.edu.sg](mailto:boredin@nus.edu.sg)

<sup>2</sup> Email: [crsccw@nus.edu.sg](mailto:crsccw@nus.edu.sg)

<sup>3</sup> Email: [scliew@nus.edu.sg](mailto:scliew@nus.edu.sg)

**KEY WORDS:** volume scattering function, Fournier-Forand, refractive index, Junge distribution

**ABSTRACT:** This paper explores the feasibility of deriving the relative refractive index and particle size distribution of coastal water samples from measurements of volume scattering functions (VSF) alone, by fitting measured VSF to the widely-used analytic Fournier-Forand (FF) scattering phase function. The FF phase function assumes a Junge-type particle size distribution and is a function of the relative refractive index and slope factor of the particle size distribution. The VSF is modeled by multiplying the total scattering coefficient to the FF phase function. The root-mean-square fractional error (RMS) between the modeled and measured VSF is used as a metric for the goodness of fit. All sets of fitting parameters that yield RMS values below a predetermined threshold are considered valid. Our results demonstrate that this approach does not return unique solutions. However, if total scattering coefficient measurements are also available, it may be possible to establish the ranges of values for the relative refractive index and slope factor.

## 1. INTRODUCTION

The relative refractive index ( $n$ ) and the particle size distribution (PSD) of the suspended particles are important quantities that provide critical information about the water and its suspended particles [Jonasz and Fournier, 2007], and can be used as inputs to radiative transfer calculations for ecosystem simulation purposes [McKee et al, 2008]. Much work has therefore been devoted to deriving these 2 quantities, especially  $n$ , which cannot be routinely measured with commercially-available instruments. However, current approaches to derive these parameters typically rely on non-optical measurements, which limit their applicability [Twardowski et al, 2001].

In this exploratory work, we investigate the use of the Fournier-Forand (FF) phase function [Fournier and Jonasz, 1999] in deriving the effective particulate refractive index,  $n$ , and the slope factor of the Junge-type PSD,  $\mu$ . The FF phase function is a relatively straightforward analytic model that assumes a Junge-type PSD and in recent years has gained popularity due to its ability to model realistic phase functions despite depending on the above 2 variables only [Haltrin, 1998]. The volume scattering function (VSF) can be modeled by multiplying the FF phase function with the total scattering coefficient  $b$ . By adjusting the three parameters,  $n$ ,  $\mu$  and  $b$ , the modeled VSF can be fitted to measured VSF using an optimization routine that minimizes the root-mean-square (RMS) fractional error between modeled and measured VSF. The main motivation of this paper is to determine if  $n$  and  $\mu$  of the suspension can be derived from VSF measurements alone, by incorporating the FF model.

## 2. BACKGROUND

The FF phase function is given by this expression [Fournier and Jonasz, 1999]:

$$P(\theta) = \frac{1}{4\pi(1-\delta)^2\delta^v} \left[ v(1-\delta) - (1-\delta^v) + [\delta(1-\delta^v) - v(1-\delta)] \sin^{-2} \left( \frac{\theta}{2} \right) \right] + \frac{1-\delta_{180}^v}{16\pi(\delta_{180}-1)\delta_{180}^v} (3 \cos^2 \theta - 1), \quad (1)$$

where  $\theta$  is the scattering angle, and

$$v = \frac{3 - \mu}{2}, \quad (2)$$

$$\delta = \frac{4}{3(n-1)^2} \sin^2\left(\frac{\theta}{2}\right). \quad (3)$$

$\delta_{180}$  denotes  $\delta$  evaluated at  $180^\circ$ . Wavelength dependence is borne by  $n$  and has been left out for clarity of presentation. The typical range of  $\mu$  is 3 to 5 [Jonasz and Fournier, 2007] while that of  $n$  is 1.0 to 1.3 [Wozniak and Stramski, 2004]. It is to be noted that the values  $\mu = 3$  and  $n = 1$  will respectively cause  $v$  and  $\delta$  to diverge and hence are avoided in the optimization procedures.

The phase function  $P(\theta)$  is related to the VSF  $\beta(\theta)$  by

$$\beta(\theta) = P(\theta)b. \quad (4)$$

where  $b$  is the total scattering coefficient. To differentiate between the measured and modelled VSF, we denote the former as  $\beta_m$  and the latter as  $\beta_{FF}$ .

### 3. METHODOLOGY

A WET Labs ECO-VSF3 three-angle, three-wavelength volume scattering function meter (VSF meter) was used to measure  $\beta(\theta)$ . The VSF meter measures  $\beta(\theta)$  at the 3 backscattering angles of  $100^\circ$ ,  $125^\circ$  and  $150^\circ$ , at 470nm, 532nm and 650nm wavelengths. Measurements were carried out at Poly Marina Singapore Polytechnic (+1.2938N, +103.7628E), a coastal location, over the period July to August 2013.  $\beta(\theta)$  was measured at different times throughout each campaign day. A comprehensive dataset was gathered over this time. However, analysis of 5 samples will be discussed for illustration. Further, we limit our current analysis to the 532nm wavelength channel.

The measured  $\beta(\theta)$  is then fitted with the modelled  $\beta(\theta)$ , by varying  $n$ ,  $\mu$  and  $b$ . For each set of these values, the RMS fractional error is calculated by

$$E_{rms} = \sqrt{\frac{\sum_i \left( \frac{\beta_{FF,i} - \beta_{m,i}}{\beta_{m,i}} \right)^2}{3}}, \quad (5)$$

where the summation is done over the 3 scattering angles mentioned above.  $n$  and  $\mu$  are constrained to the ranges pointed out in the previous section, while  $b$  is constrained to 0 to  $30 \text{ m}^{-1}$ . We first investigate the uniqueness of the optimization procedure. Instead of running the optimization over all 3 parameters at once,  $n$  is increased from 1.02 to 1.30 in steps of 0.02, and  $\mu$  from 3.01 to 5 in this sequence: 3.01, 3.2, 3.4, ... 5, so that only  $b$  is left to be optimized each time. Hence, each measured VSF  $\beta_m$  is fitted with 165 different combinations of  $n$  and  $\mu$ , with each combination returning a best-fit  $b$ . The sets of  $b$ ,  $n$  and  $\mu$  values that give  $E_{rms}$  lower than a predetermined threshold value are taken as valid solutions. We then examine the spread of the valid  $n$ ,  $\mu$  and  $b$  values to study the uniqueness of the solutions to the optimization problem.

### 4. RESULTS

Fig 1 below shows  $E_{rms}$  for samples 1 and 2 as a function of  $n$ , for various values of  $\mu$ .  $E_{rms}$  for the other samples display similar trends and values. From Fig. 1, it is clear that low values of  $\mu$  yield very poor fits to  $\beta_m$ , especially when coupled with low values of  $n$ . Less obvious is the fact that many combinations of  $n$ ,  $\mu$  and  $b$  give *equally* good fits to the data, with  $E_{rms}$  in the narrow range of 0.08 to 0.09. In fact, every step of  $n$  has a corresponding  $\mu$  and  $b$  that gives  $E_{rms}$  within this range. Since it is not possible to pick out the *one* best-fit solution based on the  $E_{rms}$ , bearing in mind that there is uncertainty in the VSF measurements, these results demonstrate that fitting the measured VSF to FF phase function alone in this optimization scheme does not return a unique solution, making this method non-feasible.

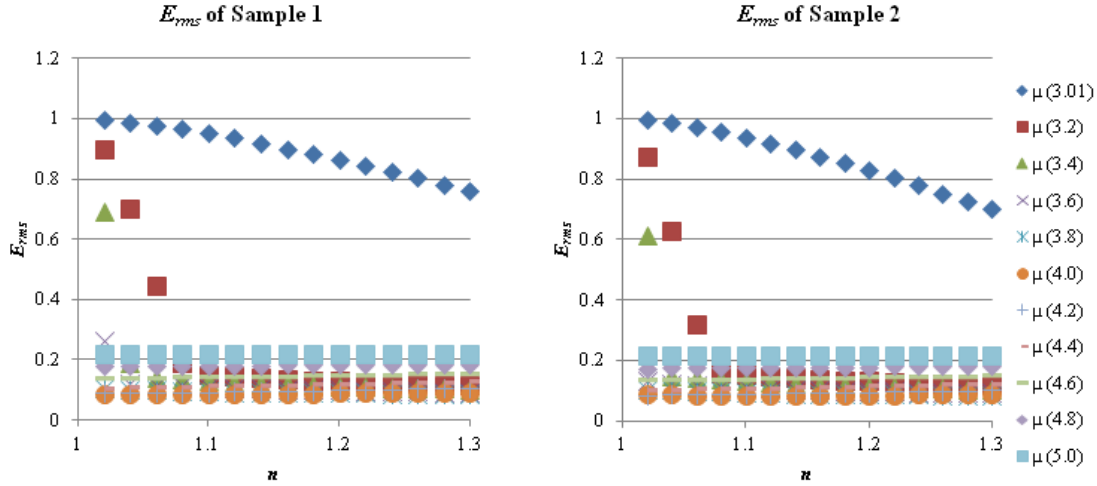


Fig 1: Variation of fitting error  $E_{rms}$  with the fitting parameters  $n$  and  $\mu$

Next, we investigate whether the non-uniqueness can be overcome by incorporating measurements of  $b$  in order to derive  $n$  and  $\mu$ . For this purpose, we have determined the threshold  $E_{rms}$  to be 0.1 based on our fitting results. All sets of fitting parameters that return  $E_{rms}$  below this value are deemed valid. For illustration, Fig. 2 shows the valid fitting parameters for fitting the measured VSF of a water sample (Sample 1 in Fig. 1) to the FF model. In this graph,  $b$  is plotted in the x-axis while  $n$  is in the y-axis for a range of valid  $\mu$  values. If  $b$  is known from measurements, it is seen that the value of  $\mu$  ranges from 3.6 to 4.2 for  $b \lesssim 2$ . For  $b$  in this range, the maximum uncertainty in  $n$  is about  $\pm 0.08$ . For larger values of  $b$ , the range of valid  $\mu$  becomes narrower since  $\mu < 3.8$  ( $\pm 0.2$ ) no longer produce valid fitting results. At  $b = 8$ , only  $\mu = 4.0$  ( $\pm 0.2$ ) is valid. The uncertainty in  $n$  is also reduced at large  $b$ . For this particular sample the measured value of  $b$  was  $4.76 \text{ m}^{-1}$ , using a WET Labs AC9 absorption-attenuation meter. Hence, from Fig. 2, the value of  $\mu$  lies in the range 3.8 to 4.2 and the value of  $n$  is estimated to be about 1.02 to 1.06.

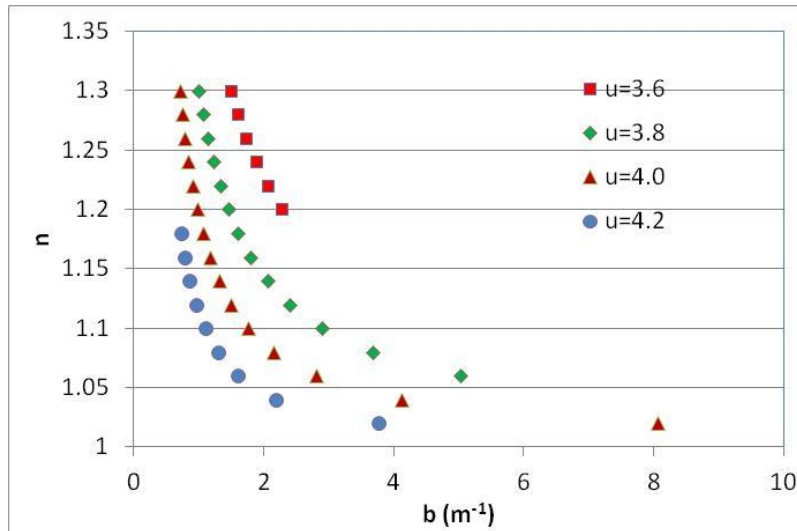


Fig 2: How  $n$  and  $\mu$  vary with  $b$ , for valid sets of fitting parameters for Sample 1

## 5. DISCUSSIONS AND CONCLUSIONS

This preliminary work has shown that although the FF phase function is a model that has its advantages, using it in such a fitting scheme to derive the relative refractive index and PSD slope factor from measurements of VSF alone is not feasible, as it returns a range of non-unique solutions. This ambiguity may be due to the fact that  $n$  and  $b$  are mutually compensating: when  $n$  is low (material has a refractive index close to that of water, hence it is not strongly

scattering), a high value of scattering coefficient  $b$  will be required to yield higher VSF, and vice versa. This would explain the generally inverse relationship between these 2 parameters as seen in Fig 2. However, our results suggest that this non-uniqueness may be partially overcome if measurements of  $b$  are also available, as this will allow us to establish the ranges where the refractive index and slope factor lie. As such, one would ideally need both measured VSF and total scattering coefficient in order to use this approach in deriving these two parameters.

## 6. REFERENCES

Fournier, G. and M. Jonasz. Computer based underwater imaging analysis. In Airborne and In-water Underwater Imaging, SPIE Vol. 3761, G. Gilbert [ed], 62-77 (1999).

Haltrin, Vladimir I. An analytic Fournier-Forand scattering phase function as an alternative to the Henyey-Greenstein phase function in hydrologic optics. Geoscience and Remote Sensing Symposium Proceedings, 1998. IGARSS'98. 1998 IEEE International. Vol. 2. IEEE, (1998).

Jonasz, M., & Fournier, G. Light scattering by particles in water: Theoretical and experimental foundations. Oxford: Academic (2007).

Woźniak, Sławomir B., and Dariusz Stramski. Modeling the optical properties of mineral particles suspended in seawater and their influence on ocean reflectance and chlorophyll estimation from remote sensing algorithms. Applied Optics 43.17 (2004): 3489-3503.

Twardowski, Michael S., et al. A model for estimating bulk refractive index from the optical backscattering ratio and the implications for understanding particle composition in case I and case II waters. *Journal of Geophysical Research: Oceans* (1978–2012) 106.C7 (2001): 14129-14142.

McKee, David, Jacek Piskozub, and Ian Brown. "Scattering error corrections for in situ absorption and attenuation measurements." Optics Express 16.24 (2008): 19480-19492.